A prospective approach for enhancing the performance of carbon-mixed concrete via retarder incorporation

Tao Meng [a,*], Haiying Yu [a], Zhejie Lai [a], Weiwei Chen [b], Shaoqin Ruan [a], Zhiguang Wang [a], Diran Yu [b]

[a] *College of Civil Engineering and Architecture, Zhejiang University, 866 Yuhangtang Road, Xihu District, Hangzhou 310058, China*
[b] *The Bartlett School of Sustainable Construction, University College London (UCL), London WCIE 6BT, UK*

ARTICLE INFO

ABSTRACT

The concrete that absorbs carbon dioxide during the mixing process, termed as carbon-mixed concrete, has become a hot research topic under the background of dual carbon goals. However, the workability of concrete significantly decreases even with the absorption of a minimal amount of carbon dioxide, indicating a potential challenge in its practical application. Therefore, this study investigated the effects of incorporating 0.5%, 1.0%, and 2.0% carbon dioxide (relative to the mass of cementitious materials) and retarder on the mechanical properties and microstructure of concrete through mercury intrusion, X-ray diffraction, and scanning electron microscopy, revealing the mechanism of retarder improving carbon-mixed concrete. The results indicated that the flowability and 28-day compressive strength of concrete mixed with 0.5% carbon dioxide decreased by 68.75% and 10.77%, respectively. However, after adding 0.25% retarder, these values for the carbon-mixed concrete only decreased by 18.75% and 3.52%. Meanwhile, the introduction of carbon dioxide can form carbonates and carboaluminates and refine the internal pores of the concrete matrix. This study proposes an effective method to improve the performance of carbon-mixed concrete, which can promote the efficient absorption of carbon dioxide in the concrete industry.

1. Introduction

Global warming, caused by the greenhouse effect, is one of the most significant environmental challenges faced by humanity today. Carbon dioxide contributes approximately 50% to the greenhouse effect, with industrial production being a major source of carbon emissions, particularly the cement manufacturing industry. The substantial energy consumption and carbon emissions of the cement industry have placed it at the center of global warming debates[1]. China, as a leading producer of cement and a major emitter of carbon dioxide, holds a prominent position in global discussions due to its high cement output and significant carbon emissions[2].

Among various Carbon Capture, Utilization, and Sequestration (CCUS) technologies, carbon dioxide mineralization in cement has become an effective technology for carbon reduction in the cement industry[3]. Currently, the application of carbon dioxide in cement-based materials can be summarized in three aspects: First is carbon dioxide curing[4], which leverages the chemical reactions between carbon dioxide and clinker components in cement to accelerate the curing process. Compared to traditional thermal curing, it not only shortens the curing time but also enhances the strength and permeability of the concrete[5,6]. The second approach involves

---

using carbon dioxide to reinforce recycled concrete aggregates(RCA)[7] and recycled cement paste powder[8,9]. In this process, carbon dioxide reacts with calcium hydroxide and hydrated calcium silicate in the cement slurry on the surface of RCA, resulting in products predominantly composed of calcium carbonate ($CaCO_3$) and silica gel. This helps refine the pore structure in the interface transition zone of the RCA[10]. The third approach is the incorporation of carbon dioxide into cement-based materials, including the direct addition of carbon dioxide or carbonates during the cement mixing process[11,12].

Specifically, in the carbon-mixed concrete(CMC) methodology, carbon dioxide is introduced during the concrete mixing process, inducing simultaneous carbonation during the hydration stage. This approach is distinct from carbon curing in cement and carbon reinforcement in aggregates, as it enables extensive contact between fresh concrete and carbon dioxide, thereby enhancing the absorption efficiency of carbon dioxide[13]. Sean Monkman et al.[14] investigated the effect of directly injecting carbon dioxide (~0.05%-0.30%) on the performance of concrete. Their findings indicated that carbon dioxide could act as an accelerant, reducing the initial setting time of concrete by up to 40% and augmenting early-stage compressive strength. This was attributed to the precipitation of nanoscale carbonate particles that served as nucleation sites for hydrated calcium silicate (C-S-H)[15]. In addition, Qian et al.[16] employed pre-carbonized cement slurry to bolster concrete performance, underscoring the carbon mixing's facilitative role in the early hydration of cement. However, carbon mixing posed challenges to the workability of concrete. Wang et al.[17] reported that the introduction of carbon dioxide mixture led to rapid hardening, and the fluidity decreased sharply with increasing carbon dioxide dosage. This was mainly related to the formation of carbonates on the surface of cement clinker.

The decrease in workability of carbon-mixed cement has emerged as a critical factor limiting both its carbon sequestration and mechanical properties[18,19]. To address this issue, researchers have attempted to disrupt the internal flocculation structure of CMC and improve its performance by adding admixtures, increasing mixing speed, and extending mixing time. Wang et al.[17] observed that extending the carbon-mixing time of cement paste by 1 minute could improve its workability by 52.8%–84.9%, due to the release of free water from the matrix. Concurrently, the early compressive strength of the cement increased by approximately 3%–15%, attributed to the deposited $CaCO_3$ promoting hydration and forming a denser microstructure. Liu et al.[20] noted a significant improvement in the flowability of carbon-mixed cement paste under ultrasonic vibration mixing compared to mechanical mixing. This method also effectively increased the rate of carbon absorption and the final absorption capacity of the cement paste. Moreover, they reported[21] that the incorporation of high-efficiency water-reducing agents could significantly enhance the fluidity of carbonated cement paste.

To address the above challenges and gaps, this study proposes a synergistic approach involving carbon dioxide and retarder to enhance the technical performance and carbon sequestration efficiency of CMC. Firstly, a specialized mixing device for CMC was designed to achieve efficient carbon absorption. Additionally, the impact of varying dosages of carbon dioxide and retarders on the mechanical properties and microstructure of concrete was investigated by X-ray diffraction and scanning electron microscopy. Finally, a hydration model for CMC based on retarder was proposed. This model provides crucial empirical data and theoretical support for a deeper understanding of the interaction between concrete and carbon dioxide. Unlike other mechanisms, the retarder extended the setting time, thereby increasing the contact time between concrete and carbon dioxide. This approach not only maintained the flowability of CMC but also enhanced the amount of carbon dioxide absorbed. It offers new insights for enhancing the technical performance of CMC, bearing significant implications for the sustainable development of the concrete industry.

2. Materials and experimental methods

2.1. Materials

The cement used in this study was Ordinary Portland Cement of the PO 42.5 grade, the chemical composition of which is shown in Table 1. The coarse aggregates included two types: crushed stone A with a particle size range of 5–31.5 mm and crushed stone B, ranging from 5 to 16 mm. Complementing these, the fine aggregates consisted of natural river sand and manufactured sand. The chemical compositions of fly ash and mineral powder are shown in Tables 2 and 3, respectively. All the above materials were supplied by Zhejiang Building Materials Group Co., Ltd. Additionally, Carbon dioxide for this research was sourced from Hangzhou Hangxiang Gas Co., Ltd. The retarder calcium lignosulfonate (CL) was provided by Zhejiang Sandu Chemical Co., Ltd. For all mixing and curing processes, tap water from Hangzhou city was utilized.

The specific mix proportions for each cubic meter of concrete were as follows: 270 kg of cement, 56 kg of mineral powder, 54 kg of fly ash, 665 kg of manufactured sand, 160 kg of natural sand, 770 kg of crushed stone A, 180 kg of crushed stone B, and 173 kg of water. The water cement ratio of concrete was 0.42.

Table 1
Chemical composition of cementitious materials.

Cementitious materials(%)	SiO_2	Al_2O_3	Fe_2O_3	CaO	MgO	SO_3	TiO_2
Cement	18.7	6.05	3.03	51.1	1.03	2.81	-
Fly ash	37.1	26.7	3.86	4.80	-	-	1.34
Mineral powder	29.6	14.9	-	33.4	9.05	1.97	-

Table 2

Mix design of CMC.

Admixture	C-0	C-0.5	CR-0.5	CR-1	CR-2
Carbon dioxide (%)	0	0.5	0.5	1	2
CL (%)	0	0	0.25	0.25	0.25

Note:"%" represents the proportion of cementitious materials.

Table 3

Porosity of the specimens.

Specimens	C-0	C-0.5	CR-0.5	CR-1.0	CR-2.0
Porosity(%)	12.94	19.77	16.23	12.55	13.68

2.2. Experimental setup

To study the effect of the concrete mixing process on carbon dioxide absorption, a novel CMC device was developed, as shown in Fig. 2. It consists of a mixer, a mixing cover, a flow meter, concentration sensor, and a pressure gauge. To ensure the airtightness of the device, a rubber pad is placed between the mixing cover and the mixer, and it is secured with bolts.

The experiment utilized both a pressure gauge and concentration sensors to determine whether there was any residual carbon dioxide gas in the mixing device. The volume of carbon dioxide introduced, V, was measured using a flow meter. Initially, upon the introduction of carbon dioxide, the readings of the pressure gauge and concentration sensors increased. After a period of mixing, their readings decreased. If both values dropped to zero and remained stable for 30 seconds, it indicated that there were no residual carbon dioxide inside the mixing device. In this experiment, the carbon dioxide absorption quantity, Q, is defined as the percentage of the mass of carbon dioxide absorbed by the concrete relative to the mass of the cementitious material, as expressed by

$$Q = \frac{\rho_0 \times V}{m_c} \tag{1}$$

Where ρ_0 refers to the density of carbon dioxide gas at standard temperature and pressure, m_c is the mass of the cementitious material (the sum of the masses of cement, fly ash, and mineral powder).

2.3. Preparation of concrete

The specific experimental steps are as follows: First, aggregate, cement, fly ash and mineral powder were poured into the mixer, and dry mixed for 30 seconds. Then, water mixed with CL was added. After the mixture was uniformly mixed, the mixing cover was placed
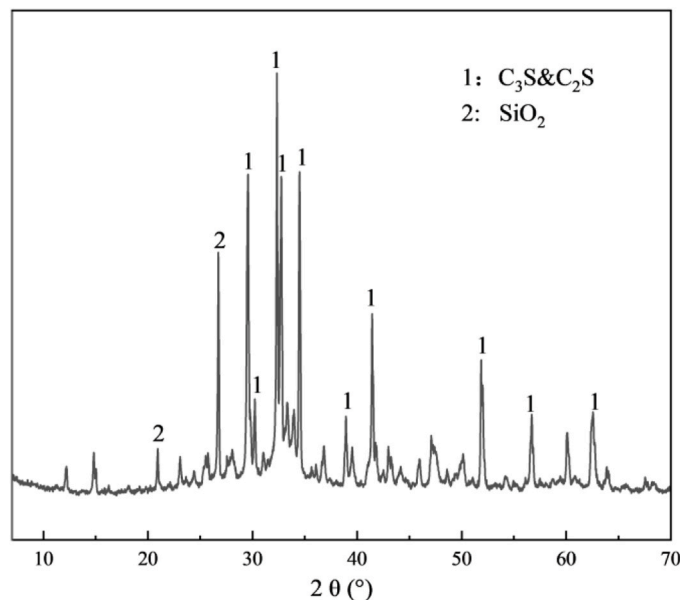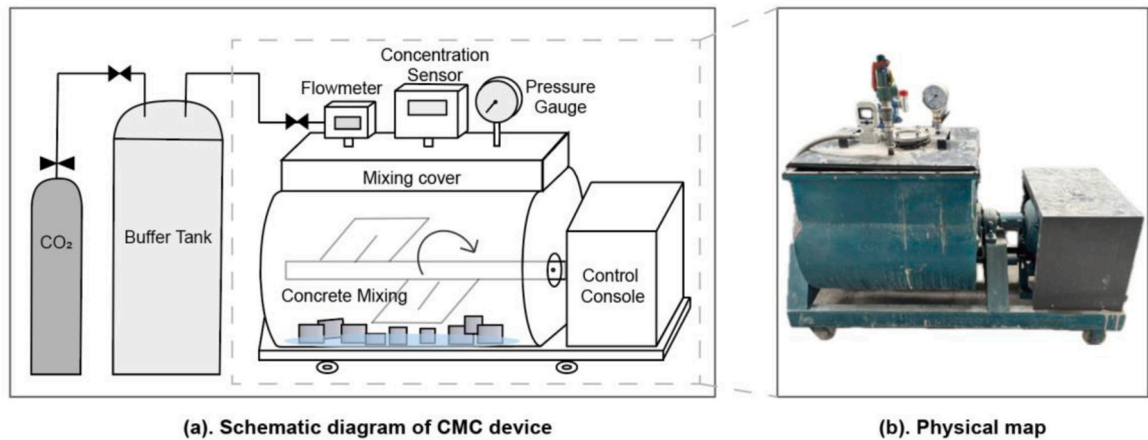

Fig. 1. XRD of cement.

Fig. 2. Schematic diagram and physical map of CMC device.

and the device was sealed with bolts. Liquid carbon dioxide was released from a pressure tank into a gas tank to convert it to carbon dioxide gas at normal temperature. Then, the carbon dioxide valve was opened, and the gas entered the concrete mixer at a certain flow rate through the flow meter. The valve was closed when the inlet flow meter reached the specified flow rate. Finally, mixing was stopped when there was no residual carbon dioxide in the mixer. Afterwards, the concrete mixer cover was opened, and the CMC was poured out for a slump test to assess its flowability.

The fresh concrete was then carefully poured into cube trial molds, each measuring 100 mm × 100 mm × 100 mm. The molds were left to stand for 24 hours, after which the concrete was demolded and placed in a standard curing room. The curing environment was stringently controlled, with the temperature set to $20\pm2°C$ and relative humidity maintained above 95%, to ensure optimal curing conditions.

2.4. Experimental methods

2.4.1. Flowability

The concrete was poured into a conical mould in the form of a frustum according to GB/T8077–2012[22]. During the test, the cone was lifted straight up to allow a free flow of the paste. The distance value from the bucket height to the highest point of concrete after the collapse was regarded as the slump of the concrete.

2.4.2. Compressive strength test

The compressive strength of the concrete was measured at 3 days, 7 days, 28 days, and 56 days using a compressive testing machine (YAW-3000B) according to GB/T50081–2019[23]. The loading speed was 0.5kN/s. For each of these time points, three individual specimens were tested to ensure the reliability and representativeness of the data.

2.4.3. Pore structure analysis

Mercury Intrusion Porosimetry (MIP) is recognized for its high precision in analyzing the micropore structure of materials. The specimens were removed from the interior of the concrete and dried at 60°C for 48 h in preparation for the MIP analysis. The MIP test was conducted using an AutoPore IV 9500, with a mercury wetting angle set at 130° and surface tension at 485 dynes/cm.

2.4.4. Thermogravimetric analysis

Thermogravimetric (TG) analysis was conducted utilizing an SDT Q600 (TA Instruments, USA). Before the test, the concrete specimens were broken and ground on a 45 mm sieve to a residue ratio of less than 2%. Each sample, weighing 10 mg, was heated at a rate of 10°C/min from 30 °C to 1000 °C, under a continuous flow of gaseous N_2 at 120 mL/min.

2.4.5. Scanning electron microscopy analysis

For the Scanning electron microscopy(SEM) analysis, the concrete specimens were broken into small fragments after the compressive strength test, and hydration was stopped using pure alcohol at a specific curing age. In addition, the sample needed to be dried for 24 hours before observing the morphology. These fragments were then gold-coated for 60 seconds using an SBC-12 Small Particles Sputtering Apparatus to enhance conductivity. The microscopic morphology of these specimens was observed under various magnifications using the Gemini SEM300.

2.4.6. X-ray diffraction analysis

X-ray Diffraction (XRD) was employed to acquire the diffraction patterns of the materials. These patterns facilitated the analysis of material composition, as well as the structure and morphology of atoms or molecules within the materials. Mineralogical

investigations were conducted via XRD analysis, utilizing an X-ray Diffraction Instrument (Bruker D8 Advance) equipped with a Cu kα X-ray radiation source. The analysis was performed with a step size of 0.026°and an acceleration voltage of 40 kV. The scanning range covered a 2θ angle from 10°to 90°.

The XRD sample was taken from the specimen after completing the compressive strength test, and then the hydration was terminated in anhydrous ethanol. It was dried in a 60 ℃ oven for 24 hours, and then the concrete sample was ground into powder using a mortar and mixed with a small amount of anhydrous ethanol. After passing through a 0.075 mm sieve, it was made into a powder sample, which can be used for the XRD test.

(a)The Slump value of concrete specimens
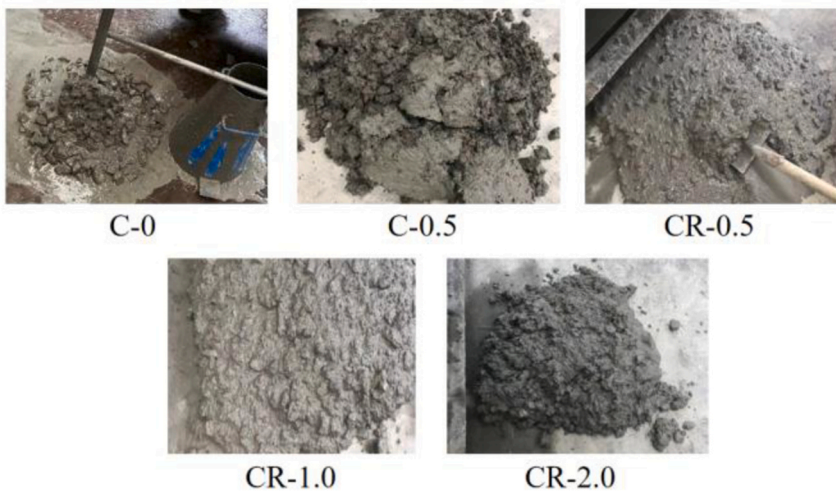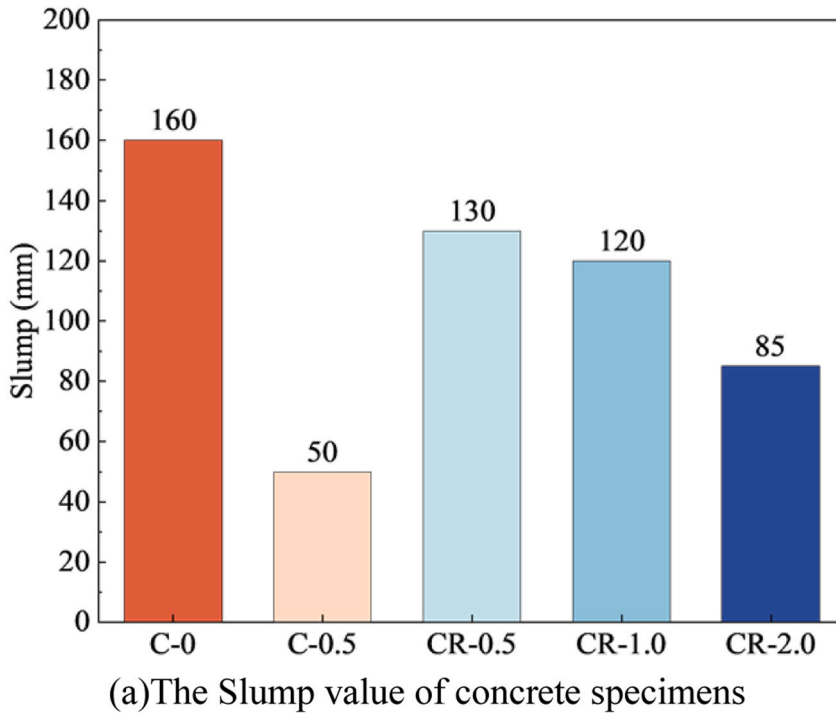
(b)The Slump test of concrete specimens

Fig. 3. The Slump value and test of concrete specimens : (a) , (b).

3. Results and discussion

3.1. Flowability

As illustrated in Fig. 3, this study investigated the impact of varying carbon dioxide contents on the flowability of concrete. The results indicated a significant reduction in concrete fluidity with the addition of carbon dioxide. Specifically, when 0.5% CO_2 was incorporated, the slump value decreased from 160 mm to 50 mm, indicating rapid setting and loss of flowability. This is because CO_2 with the calcium hydroxide (CH) generates $CaCO_3$. It is deposited on the surface of the cement particles increasing their specific surface area and thus absorbing more free water[24]. This observation aligned with the findings of Liu et al.[25], where a similar false setting phenomenon occurred in fresh cement paste absorbing 0.88% CO_2.

In the CR-0.5 group experiment, while maintaining the same CO_2 content, an additional 0.25% CL was added. This modification increased the slump value to 130 mm, which is 160% higher than the C-0.5 group, suggesting that CL enhances concrete flowability. The mixing water in fresh concrete can be categorized into four types: Adsorbed water, Hydrated water, Entrapped water, and free water, with free water being the dispersing medium[26]. CL assisted in disintegrating the flocculated structure, releasing flocculation water, thereby increasing the free water content to improve fluidity.

However, with a constant CL content, further increasing the CO_2 content to 1% led to a 7.7% decreased in slump value. When the CO_2 content was increased to 2% in the CR-2 group, the slump value dropped to 85 mm, indicating that with the increase of CO_2 content, the dosage of CL needed to be increased to meet the fluidity requirements of concrete.

3.2. Compressive strength

The compressive strength of concrete specimens with varying CO_2 content at different ages is depicted in Fig. 4. The data revealed that the incorporation of CO_2 reduced both the early and later-stage compressive strength of concrete. Compared with the C-0 benchmark group, the compressive strength of the C-0.5/CR-0.5/CR-2 group decreased by 9.39%/14.04%/19.51% at 3 days, 11.53%/10.13%/8.95% at 7 days, and 11.70%/7.60%/9.71% at 56 days, respectively. This reduction in strength could be attributed to the promotion of hydrated aluminates formation due to CO_2, leading to false setting and an increased interface porosity, as echoed by the pore characteristics discussed later. However, Liu et al.[21] found that an increase in carbon dioxide absorption had a certain reducing effect on the 7-day compressive strength of cement slurry. But as the age increases to 28 days, the compressive strength of the cement slurry after carbon absorption was higher than the reference group.

It is worth noting that compared to the experimental group with the same absorption of 0.5% carbon dioxide, the CR-0.5 group with added CL showed a 1.42% increase in 7-day strength, 7.20% at 28 days, and 4.57% at 56 days over the C-0.5 group. This improvement
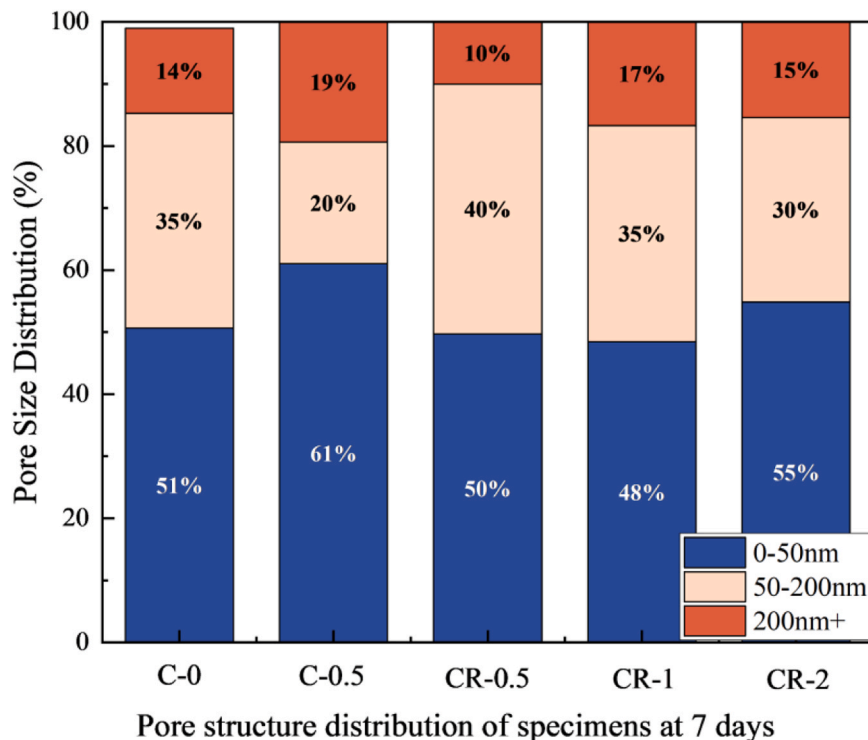

Fig. 4. Compressive strength of specimens.

was likely due to CL acting as a retarder, enhancing concrete flowability and reducing porosity, thereby increasing compressive strength. Finally, when the CO_2 content was balanced with retarder addition, CO_2 showed no significant effect on the later-stage compressive strength of concrete, as evidenced by the 0.42% increase in 56-day strength in the CR-1 group compared to the C-0 benchmark group.

3.3. Pore structure analysis

Table 3 reveals that with the carbon dioxide increasing to 0.5%, the porosity of the CMC escalates from 12.94% to 19.77%. This elevation in porosity can be attributed to rapid solidification and hardening, which subsequently decreases the matrix density. Correspondingly, it is consistent with the previously noted reduction in compressive strength for the C-0.5 group. The addition of a retarder reduced the porosity to 16.23%. Because the retarder not only delayed the setting time, mitigating the rapid setting effect induced by carbon dioxide but also enhanced the compactness of the concrete, thereby diminishing its porosity. Moreover, retarder prolonged the interaction period between the concrete and carbon dioxide, facilitating increased absorption of the gas. This promoted the formation of calcium carbonate, which filled and compacted the pore structure, thereby improving the compressive strength of the concrete with retarder compared to the reference group.

Fig. 5 shows the pore distribution of concrete specimens at different carbon dioxide dosages at 7 days. From the graph, it can be seen that there were significant differences in the influence of different amounts of carbon dioxide on the pore distribution of concrete. According to the degree of influence, it can be divided into four types: harmless pores (<20 nm), less harmful pores (20 nm~50 nm), harmful pores (50 nm~200 nm), and more harmful pores (>200 nm).

The C-0.5 group had an increase in harmless, less harmful, and more harmful pores compared to the C-0 benchmark group, while harmful pores have decreased. It suggested that CO_2 can promote the transformation of harmful pores into less harmful, harmless, and more harmful pores in early-stage concrete. Firstly, the addition of carbon dioxide led to a decrease in the workability of concrete, as well as the phenomenon of rapid setting and hardening, resulting in an increase in the proportion of more harmful pores and a decrease in the compressive strength of concrete. Simultaneously, CO_2 accelerates the formation of nanoscale $CaCO_3$[27], which fills the voids in the concrete, thereby increasing the proportion of harmless and less harmful pores.

Compared to the C-0.5 group concrete, the CR-0.5 group exhibited a transformation from more harmful pores to harmful pores. This was because CL improves the workability of concrete, resulting in a relatively dense interior and a better effect on refining pores. This may also be the reason why the compressive strength of the CR-0.5 group was higher than that of the C-0.5 group in the later stage.

In contrast, for the CR-1 group compared to the C-0 benchmark group, the proportion of harmless and less harmful pores decreased from 51% to 48%, while more harmful pores increased from 14% to 17%. As indicated by the slump values, the workability of this concrete mix was inferior to the reference group, leading to the formation of larger pores and a consequent decrease in compressive strength.

3.4. Thermogravimetric analysis

Fig. 6 depicts the thermal gravimetric (TG) and derivative thermogravimetry (DTG) curves of concrete specimens at different carbon dioxide dosages at 7days. Notably, the dehydration peaks of AFt and C-S-H gel's surface or bound water were observed between
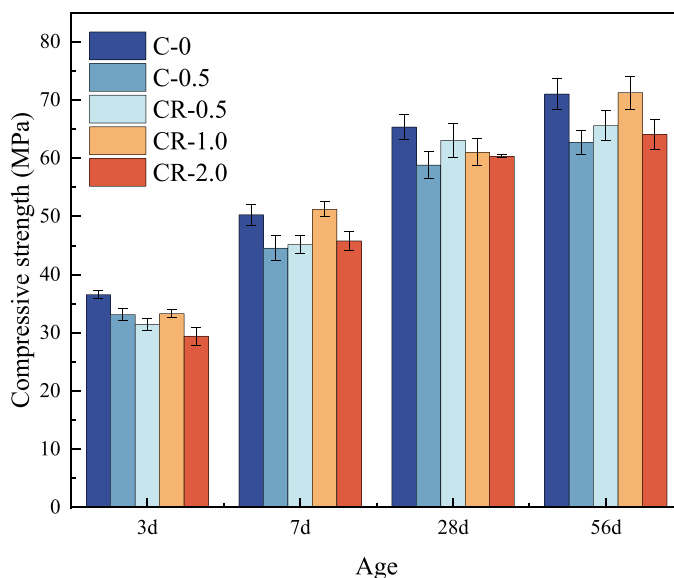

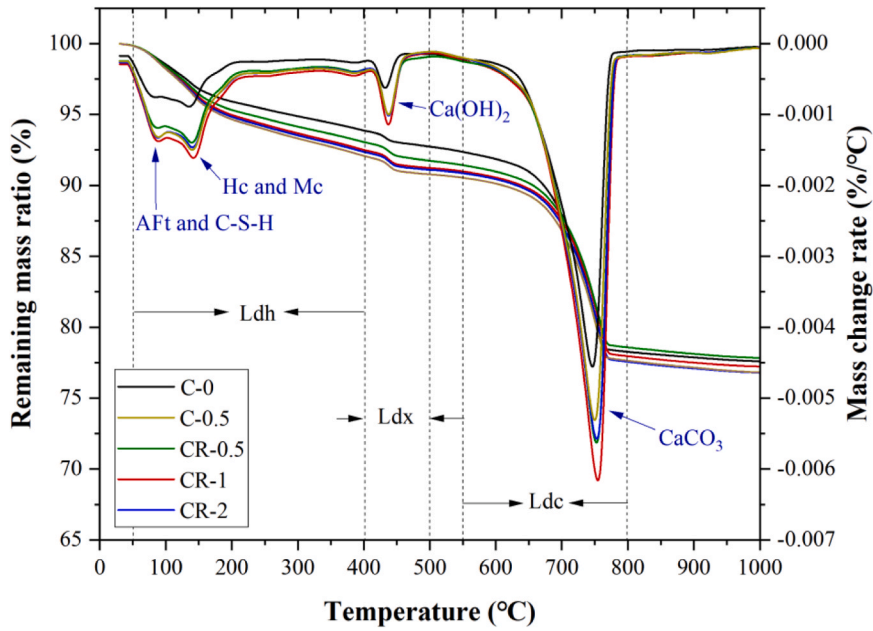**Fig. 5.** Pore structure distribution of specimens at 7 days.

Fig. 6. Derivative thermogravimetric curve (DTG) and thermalgravimetric (TG) curves of specimens at 7days.

50 and 150℃. The decomposition peaks of hemicalcium aluminate (Hc) and monocarbonate aluminate (Mc) occurred between 150 and 200℃. The weight loss between 400 and 500℃ corresponded to the decomposition of CH, and that between 550 and 800℃ was attributed to the decomposition of $CaCO_3$.

It is worth noting that for the experimental group with added carbon dioxide, the peak values of the hydration products AFt, C-S-H, and CH were much higher than those of the reference group C-0. This was precisely because carbon dioxide can promote the hydration of concrete, which was also verified in the XRD section below. Additionally, a distinct weight loss peak near 150℃ corresponded to the decomposition of Hc and Mc. In the early stage of cement hydration, tricalcium aluminate (C_3A) can react with carbonateions to form carboaluminate phases[28–30]. And it existed stably in the form of Mc, delaying the conversion of AFt to AFm.

Furthermore, post-carbonation, the $CaCO_3$ peaks were significantly higher than those in the reference group C-0. This demonstrates that carbonation during concrete mixing can lead to the formation of $CaCO_3$ within the matrix. Notably, the peak area of the calcium carbonate endothermic peak in the CR-1.0 group is the largest in each group, indicating the highest absorption of carbon dioxide. This may be because the addition of retarders slows down the hydration rate of cement and prolongs its setting time. This characteristic provides more time for the carbonation process of concrete, thereby promoting the formation of calcium carbonate. However, when the CO_2 content increased to 2%, the workability of the concrete decreased, and the setting and hardening speeds accelerated, making it difficult for more CO_2 to dissolve. Additionally, the endothermic peaks of $CaCO_3$ in the carbonation groups shifted to higher temperatures, indicating the formation of crystalline $CaCO_3$ within the sequestered carbon concrete. This conclusion aligned with the findings of Wang et al. [17].
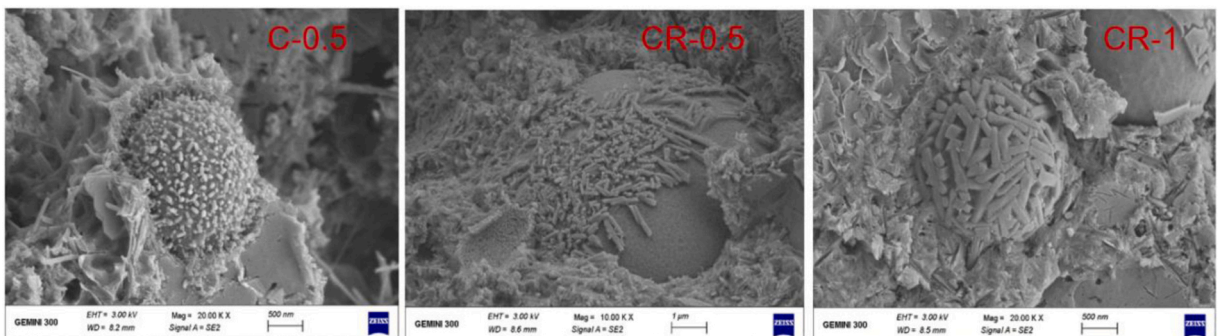

Fig. 7. SEM images of specimens at 7 days.

3.5. Scanning electron microscopy analysis

The morphology of concrete with different carbon dioxide dosages at 7 days is shown in Fig. 7. Typically, calcite exhibits rhombohedral or columnar morphologies, while aragonite, due to its different crystal structure, appears as needle-like or fibrous forms, and vaterite as spherical particles[31–33].

Previous studies[34] have reported that the surface of fly ash can physically capture carbon dioxide to promote the carbonation reaction of C_3S and C_2S. The micro-morphological images reveal that after the addition of CO_2, numerous elongated columnar crystals formed on the surface of fly ash spheres, indicating the reaction of CO_2 with the cement hydration product calcium hydroxide to form calcite. Due to its stability, calcite became the predominant crystalline form of $CaCO_3$. Furthermore, as the CO_2 content increased, the calcite crystals became more compact, enveloping the surface of the fly ash spheres. These columnar calcite crystals laid the foundation for the improvement of the late-stage compressive strength of the concrete. On the other hand, varying CO_2 contents resulted in calcite crystals with different aspect ratios, filling the surface of the hydration products and preventing further contact with CO_2.

3.6. X-ray diffraction analysis

The phase composition of concrete with different carbon dioxide contents at 7days is shown in the Fig. 8. As the CO_2 dosage increased, there was a corresponding increase in the peak height of calcite, while the peak height of calcium hydroxide decreased. This indicated that the introduction of CO_2 reacted with the calcium hydroxide to form $CaCO_3$ products. This observation was consistent with the conclusions drawn from the SEM analysis. Additionally, in the CR-2 group, the peak intensity of dolomite was significantly greater than that in the C-0 benchmark group, suggesting the formation of a larger quantity of carbonate products.

3.7. Hydration mechanism of concrete

The hydration model of concrete mixed with retarder and carbon dioxide is different from that of ordinary concrete, as shown in Fig. 9. The cement not absorbing carbon dioxide reacts with water at the initial stage of hydration to generate C-S-H gel, CH and AFt. As the hydration time continue to extend, the amount of cementitious material also increase until the cement hydration is completed.

The hydration stage of cement after adding carbon dioxide is relatively complex. Firstly, carbon dioxide is evenly dispersed in the cement slurry and dissolves first to form carbonic acid. Carbonate ions react with CH precipitated from cement hydration to form $CaCO_3$ crystals that adhere to the surface of cement particles. $CaCO_3$ particles can provide deposition sites for cement hydration products, known as nucleation effects. Part of the $CaCO_3$ reacts with C_3A to form the carboaluminate phase[35]. The reaction chemical formulas are as follows. As the absorption of carbon dioxide increases, the thickness of the $CaCO_3$ cementitious layer on the surface of cement particles increases, and the cement slurry gradually thickens, resulting in a decrease in fluidity.

Lignosulfonate can disperse cement particles by both electrostatic repulsion and steric hindrance[36]. Hydrophilic functional groups, like hydroxyl and carboxyl, enhance the wettability of the CL particles, facilitating a closer bond with the cement paste. Therefore, during carbon dioxide infusion, these hydrophilic surfaces not only promote the adherence of the cement paste to CL but also create more favorable conditions for CO_2 transfer. This enhances the concrete's active participation in the carbonation reaction, thereby increasing carbon sequestration efficiency. Ultimately, the release of entrapped water contributes to the flowability of concrete.

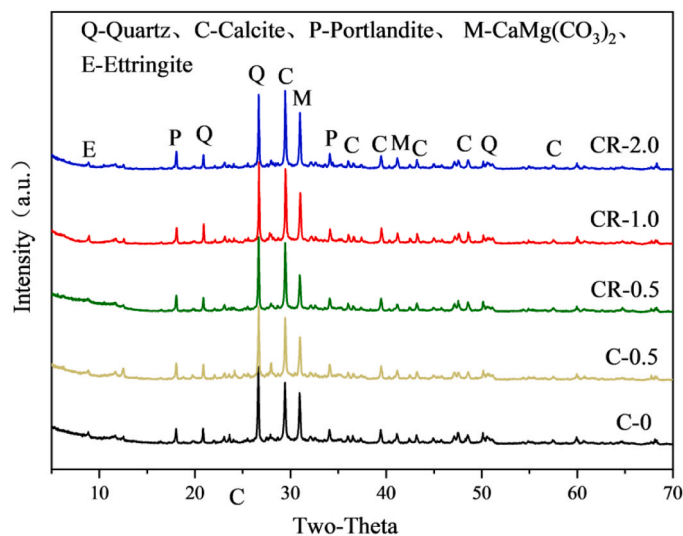The chemical formulas for cement hydration reaction after carbonization are as follow:

Fig. 8. XRD patterns of the specimens.

Fig. 9. Hydration models of concrete with or without incorporated CO_2.

$$CO_2 + H_2O \rightarrow H_2CO_3 \tag{2}$$

$$CO_2 + CH \rightarrow C\underline{C} + H_2O \tag{3}$$

$$C_3A + 0.5C\underline{C} + 0.5CH + 11.5H \rightarrow C_4A\underline{C}_{0.5}H_{12} \tag{4}$$

$$C_3A + C\underline{C} + 11H \rightarrow C_4A\underline{C}H_{11} \tag{5}$$

$$C_4A\underline{C}_{0.5}H_{12} + 0.5C\underline{C} \rightarrow C_4A\underline{C}H_{11} + 0.5CH + 0.5H \tag{6}$$

In the formula, C_3A refers to $3CaO \cdot Al_2O_3$, $C\underline{C}$ refers to $CaCO_3$, CH refers to $Ca(OH)_2$, $C_4A\underline{C}_{0.5}H_{12}$ refers to hemicalcium aluminate , $C_4A\underline{C}H_{11}$ refers to monocarbonate aluminate.

4. Conclusions

This study investigated the synergistic effect of carbon dioxide and retarder on the flowability and mechanical properties of concrete. Based on the above results and discussion, the following conclusions can be drawn:

1) The incorporation of 0.5% CO_2 significantly reduced the slump of the concrete from 160 mm to 50 mm, illustrating a rapid setting and a substantial loss of flowability. However, the addition of 0.25% calcium lignosulfonate (CL) to the mixture with the same CO_2 content successfully mitigated this effect, increasing the slump value back to 130 mm. This demonstrates the effectiveness of CL in restoring the workability of concrete affected by CO_2-induced rapid setting.
2) Compared to C-0.5, CR-0.5 demonstrated an increase in compressive strength by 1.42% at 7 days, 7.20% at 28 days, and 4.57% at 56 days. This indicates that the addition of CL is beneficial for enhancing both the early and later-stage compressive strength of CMC.
3) The addition of carbon dioxide in concrete can promote an increase in porosity. CO_2 can promote the transformation of harmful pores in CMC into more harmful pores and harmless pores. The increase in more harmful pores is a consequence of reduced concrete fluidity, which leads to the formation of larger voids. Conversely, the generation of nanoscale $CaCO_3$ acts to fill the smaller pores, mitigating their harmful impact.

CRediT authorship contribution statement

Shaoqin Ruan: Supervision, Writing – review & editing, Visualization. **Zhiguang Wang:** Supervision, Resources. **Zhejie Lai:** Investigation, Data curation. **Weiwei Chen:** Software, Investigation. **Diran Yu:** Supervision. **Haiying Yu:** Writing - review & editing, Formal analysis, Writing – original draft, Formal analysis. **Tao Meng:** Writing – original draft, Methodology, Funding acquisition, Conceptualization.

Declaration of Competing Interest

The authors declare that they have no known competing financial interests or personal relationships that could have appeared to influence the work reported in this paper.

Data Availability

Data will be made available on request.

References

[1] C. Shi, B. Qu, J.L. Provis, Recent progress in low-carbon binders, Cem. Concr. Res. 122 (2019) 227–250, https://doi.org/10.1016/j.cemconres.2019.05.009.
[2] R.M. Andrew, Global CO_2 emissions from cement production, 1928–2018, Earth Syst. Sci. Data 11 (2019) 1675–1710, https://doi.org/10.5194/essd-11-1675-2019.
[3] Z. Liu, W. Meng, Fundamental understanding of carbonation curing and durability of carbonation-cured cement-based composites: a review, J. CO_2 Util. 44 (2021) 101428, https://doi.org/10.1016/j.jcou.2020.101428.
[4] J.G. Jang, G.M. Kim, H.J. Kim, H.K. Lee, Review on recent advances in CO2 utilization and sequestration technologies in cement-based materials, Constr. Build. Mater. 127 (2016) 762–773, https://doi.org/10.1016/j.conbuildmat.2016.10.017.
[5] J.G. Jang, H.K. Lee, Microstructural densification and CO2 uptake promoted by the carbonation curing of belite-rich Portland cement, Cem. Concr. Res. 82 (2016) 50–57, https://doi.org/10.1016/j.cemconres.2016.01.001.
[6] D. Zhang, Z. Ghouleh, Y. Shao, Review on carbonation curing of cement-based materials, J. CO2 Util. 21 (2017) 119–131, https://doi.org/10.1016/j.jcou.2017.07.003.
[7] B.J. Zhan, C.S. Poon, C.J. Shi, Materials characteristics affecting CO2 curing of concrete blocks containing recycled aggregates, Cem. Concr. Compos. 67 (2016) 50–59, https://doi.org/10.1016/j.cemconcomp.2015.12.003.
[8] M. Zajac, J. Skocek, P. Durdzinski, F. Bullerjahn, J. Skibsted, M. Ben Haha, Effect of carbonated cement paste on composite cement hydration and performance, Cem. Concr. Res. 134 (2020) 106090, https://doi.org/10.1016/j.cemconres.2020.106090.
[9] Y. Mao, S. Drissi, P. He, X. Hu, J. Zhang, C. Shi, Quantifying the effects of wet carbonated recycled cement paste powder on the properties of cement paste, Cem. Concr. Res. 175 (2024) 107381, https://doi.org/10.1016/j.cemconres.2023.107381.
[10] C. Liang, B. Pan, Z. Ma, Z. He, Z. Duan, Utilization of CO2 curing to enhance the properties of recycled aggregate and prepared concrete: a review, Cem. Concr. Compos. 105 (2020) 103446, https://doi.org/10.1016/j.cemconcomp.2019.103446.
[11] S. Monkman, Y. Sargam, O. Naboka, B. Lothenbach, Early age impacts of CO2 activation on the tricalcium silicate and cement systems, J. CO2 Util. 65 (2022) 102254, https://doi.org/10.1016/j.jcou.2022.102254.
[12] S. Monkman, M. MacDonald, On carbon dioxide utilization as a means to improve the sustainability of ready-mixed concrete, J. Clean. Prod. 167 (2017) 365–375, https://doi.org/10.1016/j.jclepro.2017.08.194.
[13] N. Lippiatt, T.-C. Ling, S. Eggermont, Combining hydration and carbonation of cement using super-saturated aqueous CO2 solution, Constr. Build. Mater. 229 (2019) 116825, https://doi.org/10.1016/j.conbuildmat.2019.116825.
[14] S. Monkman, M. MacDonald, R.D. Hooton, P. Sandberg, Properties and durability of concrete produced using CO2 as an accelerating admixture, Cem. Concr. Compos. 74 (2016) 218–224, https://doi.org/10.1016/j.cemconcomp.2016.10.007.
[15] S. Monkman, Y. Sargam, L. Raki, Comparing the effects of in-situ nano-calcite development and ex-situ nano-calcite addition on cement hydration, Constr. Build. Mater. 321 (2022) 126369, https://doi.org/10.1016/j.conbuildmat.2022.126369.
[16] X. Qian, J. Wang, Y. Fang, L. Wang, Carbon dioxide as an admixture for better performance of OPC-based concrete, J. CO2 Util. 25 (2018) 31–38, https://doi.org/10.1016/j.jcou.2018.03.007.
[17] M. Wang, S. Luo, B.T. Pham, T.-C. Ling, Effect of CO2-mixing dose and prolonged mixing time on fresh and hardened properties of cement pastes, J. Zhejiang Univ. Sci. A 24 (2023) 886–897, https://doi.org/10.1631/jzus.A2200571.
[18] S. Luo, M.-Z. Guo, T.-C. Ling, Mechanical and microstructural performances of fly ash blended cement pastes with mixing CO2 during fresh stage, Constr. Build. Mater. 358 (2022) 129444, https://doi.org/10.1016/j.conbuildmat.2022.129444.
[19] N. Lippiatt, T.-C. Ling, Rapid hydration mechanism of carbonic acid and cement, J. Build. Eng. 31 (2020) 101357, https://doi.org/10.1016/j.jobe.2020.101357.
[20] L. Liu, Y. Ji, Z. Ma, F. Gao, Z. Xu, Study on the effects of ultrasonic agitation on CO2 adsorption efficiency improvement of cement paste, Appl. Sci. 11 (2021) 6877, https://doi.org/10.3390/app11156877.
[21] L. Liu, Y. Ji, F. Gao, L. Zhang, Z. Zhang, X. Liu, Study on high-efficiency CO2 absorption by fresh cement paste, Constr. Build. Mater. 270 (2021) 121364, https://doi.org/10.1016/j.conbuildmat.2020.121364.
[22] China National Standards GB/T8077-2012, Methods for testing uniformity of concrete admixture, Beijing, China (in Chinese).
[23] China National Standards GB/T50081-2002, Standard for test method of mechanical properties on ordinary concrete, Beijing, China (in Chinese).
[24] K. Cui, D. Lau, Y. Zhang, J. Chang, Mechanical properties and mechanism of nano-CaCO3 enhanced sulphoaluminate cement-based reactive powder concrete, Constr. Build. Mater. 309 (2021) 125099, https://doi.org/10.1016/j.conbuildmat.2021.125099.
[25] X.Liu, Research of the Hydration and Hardening Mechanism of Cement-Based Materials after Absorbing CO2 in Mixing Stage. MS Thesis, China University of Mining and Technology, 2019, China (in Chinese).
[26] E. Cao, Y. Zhang, X. Kong, The microstructure model of fresh cement paste with superplasticizer, Concrete (8) (2012) 37–161.
[27] S. Monkman, P. Kenward, G. Dipple, Physicochemical impacts of in-situ mineralized CaCO3 on very early hydration of cement at two temperatures, ACS Sustain. Chem. Eng. 11 (2023) 6261–6271, https://doi.org/10.1021/acssuschemeng.2c07480.

[28] A. Ipavec, R. Gabrovšek, T. Vuk, V. Kaučič, J. Maček, A. Meden, Carboaluminate phases formation during the hydration of calcite-containing portland cement: carboaluminate phase formation, J. Am. Ceram. Soc. 94 (2011) 1238–1242, https://doi.org/10.1111/j.1551-2916.2010.04201.x.

[29] B. Lu, C. Shi, J. Zhang, J. Wang, Effects of carbonated hardened cement paste powder on hydration and microstructure of Portland cement, Constr. Build. Mater. 186 (2018) 699–708, https://doi.org/10.1016/j.conbuildmat.2018.07.159.

[30] Y. Zhang, X. Zhang, Research on effect of limestone and gypsum on C3A, C3S and PC clinker system, Constr. Build. Mater. 22 (2008) 1634–1642, https://doi.org/10.1016/j.conbuildmat.2007.06.013.

[31] K. Garbev, P. Stemmermann, L. Black, C. Breen, J. Yarwood, B. Gasharova, Structural features of C–S–H(I) and its carbonation in air—a Raman spectroscopic study. Part I: fresh phases, J. Am. Ceram. Soc. 90 (2007) 900–907, https://doi.org/10.1111/j.1551-2916.2006.01428.x.

[32] H. Yu, C. Tang, H. Mehdizadeh, M.-Z. Guo, T.-C. Ling, Effects of early hydration of alite and belite phases on subsequent accelerated carbonation, Constr. Build. Mater. 411 (2024) 134675, https://doi.org/10.1016/j.conbuildmat.2023.134675.

[33] F. Wu, X. You, M. Wang, T. Liu, B. Lu, G. Hou, R. Jiang, C. Shi, Increasing flexural strength of CO2 cured cement paste by CaCO3 polymorph control, Cem. Concr. Compos. (2023) 105128, https://doi.org/10.1016/j.cemconcomp.2023.105128.

[34] J.F. Young, R.L. Berger, J. Breese, Accelerated curing of compacted calcium silicate mortars on exposure to CO2, J. Am. Ceram. Soc. 57 (1974) 394–397, https://doi.org/10.1111/j.1151-2916.1974.tb11420.x.

[35] Z. Tu, M. Guo, C.S. Poon, C. Shi, Effects of limestone powder on CaCO3 precipitation in CO2 cured cement pastes, Cem. Concr. Compos. 72 (2016) 9–16, https://doi.org/10.1016/j.cemconcomp.2016.05.019.

[36] H.V. Vikan, Rheology and Reactivity of Cementitious Binders with Plasticizers, Doctoral thesis, Fakultet for naturvitenskap og teknologi, 2005. https://ntnuopen.ntnu.no/ntnu-xmlui/handle/11250/244516 (accessed March 6, 2024).